Article

A novel method of creating thermoplastic chitosan blends to produce cell scaffolds by FDM additive manufacturing

Robert Tylingo[1#], Piotr Kempa[2], Adrianna Banach-Kopeć[1], Szymon Mania[1#*]

[1] Chemical Faculty, Department of Chemistry, Technology and Biotechnology of Food, Gdansk University of Technology, 11/12 G. Narutowicza Str., 80-233 Gdansk, Poland; robertt@pg.edu.pl (R.T.), adrianna.banach@pg.edu.pl (A.B-K.), szymon.mania@pg.edu.pl (S.M.)

[2] Chitone Sp. z o. o. 15 Pionierów Str., 84-300 Lębork, Poland; p.kempa@chitone.pl (P.K.)

*Correspondence: szymon.mania@pg.edu.pl, Tel.: +48-58-347-28-56

Abstract:

Due to its remarkable and promising biological and structural properties, chitosan has been widely studied in several potential applications in the biomedical sector. Attempts are being made to use this polymer and its properties in thermoplastics dedicated to 3D printing in FDM technology. However, chitosan can be processed only from acid solution, which limits its applications.The paper presents a new path for the production of filaments based on unstable chitosan hydrogels obtained by carbon dioxide saturation, as well as synthetic polymers such as polyvinyl alcohol and polycaprolactone. The results confirm that the absence of acid allows formation of thermally stable and printable filaments containing from 5% to 15% of chitosan, capable of reducing *S. aureus* and *E. coli* bacteria by 0.41-1.43 in logarithmic scale (56 – 94%) and 0.28-0.94 in logartithimc scale (36 – 89%), respectively.

Keywords: 3D printing; chitosan; polycaprolactone; filament; antimicrobial properties

1. Introduction

Creating polymer compositions by physical mixing or chemical coupling is one of the most popular ways of producing materials with novel properties. These properties may correlate with the concentration of components present in the created composites or give them completely new and non-obvious features (Rajeswari, Sreerag Gopi, Jackina Stobel Christy Jayaraj, & Pius, 2020). Polymers from renewable sources deserve particular attention because of their low cost, high availability, non-toxicity and ability to be used in products from sustainable resources. Chitosan (CS) is an example of such a resource. Chitosan is the product of chitin deacethylation, composed of randomly distributed ß(1→4)-linked D-glucosamine and N-acetyl-D-glucosamine units in a linear polymer structure. The sources of chitin are exoskeletons of shellfish and insects, as well as the cell walls of fungi (Muzzarelli, 2009). Due to its biocompatibility, biodegradability, antimicrobial properties, non-toxicity, and film-forming properties, chitosan offers potential in a range of applications (Rinaudo, 2006).The major challenge in the efficient production of renewable polymers is the compatibility of the raw material with common industrial processing methods such as extrusion, injection moulding and extrusion blow moulding. Over the last few years, the meltability of thermoplastic polymers has been strongly focused on the versatility of production by 3D printing

# These authors contributed equally to this paper.

40 methods with a particular focus on the fused deposition method (FDM), which is based on creating

41 three-dimensional products by melting the raw material and depositing it on previously produced

42 layers of solidified material (Mania, Banach, & Tylingo, 2020). Despite a number of advantages, the

43 use of chitosan in the above methods is very limited as it does not melt. Therefore, obtaining

44 composites with biological properties resulting from the characteristics of intempersible

45 biopolymers, such as antimicrobial activity, is still very restricted.

46　　In the scientific literature, there are examples of studies that attempted to overcome this

47 limitation. The simplest methods are the use of additives of chitosan or other biopolymers as a solid

48 material in the form of particles in the polymer matrix, which guarantees the meltability of the

49 material (Bonilla, Fortunati, Vargas, Chiralt, & Kenny 2013; Correlo et al., 2009). This solution is

50 effective when chitosan, as a filler, is used in concentrations of 0.5 - 1.5% (Rojas-Martínez et al.,

51 2020). Our previous work has shown that direct co-extrusion of chitosan with a poly(lactic acid)

52 (PLA) matrix hinders the achievement of homogeneous and smooth 3D printing filaments. The

53 filaments containing more than 3% of chitosan in PLA matrix were not suitable for FDM printing and

54 had weak antimicrobial properties (Mania et al., 2019).

55　　Epure et al. have modified the physicochemical properties of chitosan to make it thermoplastic.

56 Chitosan in powder form was mixed with glycerol and 2% acetic acid was added to form a plastic

57 paste which was pressed hot. The addition of glycerol made the product extendable and therefore it

58 did not crumble (Epure, Griffon, Pollet, & Avérous, 2011). However, it was not possible to

59 completely melt the chitosan and the final colour of the mixture was darkened in the presence of

60 acetic acid.

61　　Grande, Pessan and Carvalho (2015) proposed a method of obtaining a plastic chitosan

62 composite with PLA. It consisted of mixing 1% chitosan solution in acetic acid with 1% poly(vinyl

63 alcohol) (PVA) solution as a compatibility enhancer and using glycerol as a plasticizer (Grande,

64 Pessam, & Carvalho, 2015). The mixture was gently dried, ground and re-dried and then mixed with

65 PLA granules. The method developed made it possible to obtain thermoplastic filaments but did not

66 solve the problem of polymer degradation, which results from the residual acid used to dissolve the

67 chitosan. The authors indicated severe degradation of chitosan and of PLA leading to a decrease in

68 the mechanical properties and strong darkening during processing, even when the PVA-chitosan

69 blend was dried at mild temperatures (<50°C). Thus, the extraction of acid residues proved to be an

70 obstacle to overcome.

71　　Other research groups have also worked on obtaining thermoplastic chitosan using polyols,

72 water and acetic acid as an alternative to the thermomechanical method (Dang & Yoksan, 2015;

73 Mendes et al., 2016). Although this approach reduced the size of the dispersed chitosan phase to a

74 few microns, the irregular geometry of the dispersed phase indicated that chitosan was not

75 effectively melted during thermo-mechanical mixing. Unfortunately, the problem of the darkening of

76 the resulting mixtures has still not been solved and has intensified with the increase in chitosan

77 concentration in composites (Matet, Heuzey, Pollet, Ajji, & Avérous, 2013).

78　　 Grande, Pessan and Carvalho (2018) suggested a way to obtain thermoplastic PLA, PVA and

79 chitosan blends. The first stage consisted of mixing a 1% solution of PVA and a 1% solution of

80 chitosan in 1% acetic acid, which was then spray-dried, while the volatile acetic acid at the drying

2

81   temperature was driven away together with water. Another way was to freeze the mixture of

82   solutions and subject it to freeze-drying. However, it must be taken into account that the

83   evaporation of acetic acid from the material during sublimation may not always be efficient and may

84   result in increased exploitation of the apparatus on an industrial scale (Grande, Pessan, &

85   Carvalho, 2018). Target composites presented by the authors contain from 2.5 to 6.25% chitosan

86   and the studies do not present the effect of long-term processing of the composite at extrusion

87   temperature.

88   In in our work, we tried to confirm the hypothesis that the elimination of acid during chitosan

89   dissolution will allow obtaining thermoplastic and thermostable filaments in a PCL matrix with

90   antimicrobial activity. This effect was attempted by using an innovative method of saturation with

91   gaseous carbon dioxide for the processing of chitosan in the form of a solution. To date, such an

92   approach to obtain thermoplastic chitosan composites has not been proposed in the scientific

93   literature.

2. Experimental methods

2.1. Materials

96   Medium molecular weight chitosan (MMW) with deacetylation degree of 81-96% was

97   purchased from Primex (Iceland). PVA with molecular weight of 9-10 kDa and a degree of

98   hydrolysis of 80% was purchased from Merck (Germany). Medium molecular weight PCL with a

99   melting index equal to 11 g/10 min at 100°C was purchased from Esun Industrial Co., Ltd.

100   (Shenzhen, China). The acetic acid, hydrochloric acid and sodium hydroxide were produced by

101   Avantor Performance Materials Poland S.A (Gliwice, Poland). The carbon dioxide used to saturate

102   the chitosan preceipitate was derived from Linde Gaz Polska Sp. z o. o. (Gdańsk, Poland). For

103   microbiological tests, the following bacterial strains were used: Gram (−) *Escherichia coli* (ATCC

104   25922) and Gram (+) *Staphylococcus aureus* (ATCC 29213) from the Polish Collection of

105   Microorganisms, Ludwik Hirszfeld Institute of Immunology and Experimental Therapy of the Polish

106   Academy of Sciences (Wrocław, Poland). Phosphate Buffered Saline (PBS), Tryptic Soy Agar

107   (TSA), and Tryptic Soy Broth (TSB) media were purchased from Merck (Germany).

2.2. Preparation of CS/PVA composites

109   Chitosan/poly(vinyl alcohol) (CS/PVA) composites were made in three variants: 1% CS solution

110   in 0.1M acetic acid, 1% CS solution in 0.1M hydrochloric acid, and 1% CS solution in carbonic acid.

111   The 1% CS solution in 0.1M acetic acid and 0.1M hydrochloric acid was obtained by indirect

112   dissolving of polymer in acid solution under mechanical stirring at a speed of 300 RPM (RA 2020,

113   Heidolph Instruments GmbH & Co. KG, Kelheim, Germany) until a homogenous and clear solution

114   was obtained (3 hours). The 1% chitosan solution in carbonic acid (CS-CO_2) was prepared

115   according to the methodology proposed by Gorczyca and colleagues with slight modifications

116   (Gorczyca et al., 2014).

117   In the first step, 1.5% CS solution in 0.1M acetic acid was obtained by indirect dissolution of

118   polymer in proper acid solution during mechanical stirring at a speed of 300 RPM (RA 2020,

119   Heidolph Instruments GmbH & Co. KG, Kelheim, Germany). Then, during mixing, 0.5M solution of

120   sodium hydroxide was added until a pH value in the range of 9-10 was reached. This was

121   equivalent to complete precipitation of chitosan in the microcrystalline form. The precipitated

3

chitosan was filtered with the use of a seepage kit under reduced pressure and was washed several times with distilled water until the pH of the rinsing water reached a value equal to 7.0. Finally, the precipitated chitosan was weighed and suspended in such an amount of distilled water to obtain a solution of 1 % in relation to the dry matter of the polymer. The CS suspension was homogenized at 10000 RPM for 3 minutes (Silent Crusher M, Heidolph Instruments GmbH & Co. KG, Kelheim, Germany) and then saturated with CO_2 with simultaneous mechanical mixing using a hollow shaft stirrer for gas saturation (BIOMIXBMX-10, Gdańsk, Poland) until completely dissolved.

The PVA solution was made by heating distilled water to 60°C and adding to it small portions of the appropriate amount of PVA to obtain a concentration of 1%. The mixture was strongly mixed with simultaneous heating to 50-60°C (MR Hei-Standard, Heidolph Instruments GmbH & Co. KG, Kelheim, Germany). After obtaining a homogeneous solution, it was cooled to room temperature. The finished PVA solution and chitosan solution dissolved in hydrochloric or acetic or carbonic acid were mixed at a 1:1 mass ratio, frozen at -24°C and then freeze-dried for 72 h (p = 0.94 mbar, sample temperature 20°C, condenser temperature -80°C; Christ Alpha 12–4 LD Plus, Osterode am Harz, Germany).

2.3. Evaluation of the effect of extrusion time on the colour of CS/PVA composite

Freeze-dried PVA/chitosan composites were ground in a laboratory mill (ChemLand, FW 135, Stargard, Poland) to obtain fine chips (approx. 5 s). The crushed material was placed in glass petri dishes with lids, which were then placed in a laboratory oven heated to 150°C (BINDER FDL 115, Gmbh, Tuttlingen, Germany). The process of heating the composites was carried out for 4 hours. The results were presented in the form of photos of the composites taken before heating and after 1, 2, 3 and 4 hours of heating (Nikon D7200 camera (Kumagaya, Japan).

2.4. Filament preparation

To produce thermoplastic filaments based on chitosan, poly(vinyl alcohol) and polycaprolactone, in the first stage CS-CO_2/PVA composites were prepared by mixing 1% CS-CO_2 solution and 1% PVA solution in 3:1, 1:1, 1:3 mass ratios and freeze-drying for 72 hours (p = 0.94 mbar, sample temperature 20°C, condenser temperature -80°C; Christ Alpha 12–4 LD Plus, Osterode am Harz, Germany). The dry CS-CO_2/PVA composites were ground in a laboratory mill (ChemLand, FW 135, Stargard, Poland), until a fine powder was obtained. Prior to the extrusion process, an extruder was started (Wellzoom C, Zhenzen, China), setting a temperature of 150°C in the dosing and extrusion zone. When the temperature was reached, the milled material was placed in the dispenser of the extruder and the dosing auger drive was started. The extrusion process was carried out at a speed of 2000 mm/min. The molding nozzle diameter was equal to 1.75 mm. The resulting extrudate was cut by hand into sections not exceeding 3 mm in length. The CS-CO_2/PVA/PCL filaments were produced by mixing 80g of PCL granules and 20g of selected CS-CO_2/PVA composite granules and extrusion. The thoroughly mixed combination was then re-extruded using the same extruder and the same extrusion conditions as were used to produce granules of the CS-CO_2/PVA composites.

2.5. 3D Print Preparation

The CAD model in the form of a 12.5 mm diameter and 20 mm high cylinder was created with AutoCAD 2019 software and exported in "stl" format. The file was converted to "gcode" using Z-

4

Suite V 2.12.0.0 software. The object was printed using the FDM technique with a Zortrax M200 Plus printer (Olsztyn, Poland) with working space dimensions 200 x 200 x 300 mm. Printing parameters for control (PCL) and CS-CO$_2$/PVA/PCL filaments were as follows: extruder nozzle size 0.4mm, layer height 0.1mm, print filling: 30%, print temperature: 150°C, working field temperature: 30°C.

2.6 Material characterization

2.6.1 Morphological evaluation (SEM)

The topography of the filaments was evaluated using a VP-SEM S3400-N scanning electron microscope (Hitachi, Hyogo, Japan). The acceleration voltage was 25 kV. Compensation of the charge was ensured by recording the images at a vacuum of 120 Pa and using a back-scattering electron detector (BSE). The use of the BSE detector allowed increase of the contrast of local areas differing in mass and/or density of the material. Visual recording of the samples was obtained with Nikon D7200 (Warsaw, Poland).

2.6.2. Chemical structure (FTIR)

FT-IR spectra have been recorded using a spectrometer (Nicolet 8700; Thermo Electron Corp., Waltham, MA, USA) equipped with GoldenGate (Specac Corp., Oprington, UK) with a single-reflection diamond. The temperature of the crystal was maintained at 25.0 ± 0.1°C during measurement. 64 scans were obtained with a resolution of 4 cm^{-1} within the wavelength range from 4000 to 550 cm^{-1}. The spectrum of each material was measured, averaged and corrected by background removal. Spectragryph V software was used to process the obtained spectra. 1.2.10 (Oberstdorf, Germany).

2.6.3. Thermal stability (TGA)

A thermogravimetric analyser (TA Instruments SDT 600, Warsaw, Poland) was used to measure the change in weight of the sample due to decoposition. During the measurement, the samples were heated at a constant rate of 10°C/min between 30°C and 800°C. The tests were conducted in a nitrogen atmosphere.

2.6.4. Mechanical properties and printability

The mechanical properties were tested using a universal testing machine (Instron model 5543 with "Merlin" V 4.42. software, Warsaw, Poland). Filaments were tested in accordance with ISO 527: 2012. The filaments were cut into 10 cm lengths and conditioned in an air climatic chumber at 25°C for 24 hours under relative humidity equal to 50%. In order to perform the measurement, each of the filaments was mounted in the jaws of the apparatus so that the length of the measurement section was 50 mm. The speed of the head movement causing the filament stretching was 100 mm/min. Each test was performed in 10 replicates. Based on the diagram of the relationship between breaking stress and deformation, test parameters such as tensile strength, strain at break and Young's modulus were determined. The printability of the filaments was assessed by the toughness parameter measurement in the indirect instrumental stiffness test proposed by Xu et others: kg/mm2*%, pressure unit expressed as a percentage and used to describe the mechanical parameters of tests using texture analysis methods (Xu et al., 2020). The universal testing machine

5

was equipped with a three-point-bending rig with thin blades (3 mm thickness). The filament was cut into 6 cm in length and placed on top of the machine platform. Trigger force was set to 50 g, and the blade was set to cut the filament until 1 mm in distance (57% strain) at a speed of 2 mm/s. The maximum force and fracture distance were recorded by Merlin software. Based on the area under the curve and maximum stress, the toughness parameter was calculated. The mechanical properties of the cylindrically shaped 3D prints were characterized according to the method described by Bi and Hoyer with co workers with slight modifications (Bi et al., 2011; Hoyer et al., 2012). Five cylindrical samples (Ø 12.5 mm h=20 mm) were compressed up to 10% deformation in two cycles at a test speed of 0.5 mm/s. The hardness, flexibility, and cohesiveness were measured. Hardness was determined as the ratio of the maximum force in the first compression cycle to the compressed surface. Elasticity is a dimensionless quantity expressed as the ratio of the distance of the pin compressing the sample from the beginning of compression to the achievement of the maximum force in the second cycle with the same distance determined in the first cycle. Cohesiveness, also a dimensionless value, was determined as the ratio of the area under the curve in the second compression cycle to the area under the curve in the first compression cycle.

2.6.5. Antimicrobial activity

The evaluation of antimicrobial properties of the materials was performed according to the ASTM E2149 method with slight modification using *E. coli* and *S. aureus* strains. Colonies of bacteria were first subcultured to triptic soya broth and incubated for 24 h at 37°C. Then microbial suspensions were diluted in phosphate buffered saline to obtain a number of bacterial cells between 1.5×10^7 to 5×10^7 CFU/mL. Dillutions were made with a spectrophotometer by measuring the absorbance at 600 nm wavelengths (optical density $0.08 \div 0.1$). Antimicrobial activity tests were conducted for CS-CO_2/PVA composites, CS-CO_2/PVA/PCL filaments, and 3D prints.

To determine the antimicrobial activity of CS-CO_2/PVA composites, squares with 5 cm edge length were cut out of the composites and PE film (negative control without the antimicrobial properties). Then square samples were sterilised under UV radiation (30 minutes on each side). Afterwards, 0.4 mL of inoculum containing 1.5×10^7 to 5×10^7 CFU/mL of tested bacterial strain was applied to each of the square. The inoculated samples were covered with sterile square-shaped PE foils with an edge length of 4 cm to ensure proper contact of the bacterial suspension with the tested material (16 cm^2). The samples prepared in this way were incubated 24 hours at 37°C (Heidolph Incubator 1000, Merck Sp. z o.o., Warsaw, Poland). After incubation each sample was transferred to 10 mL PBS solution and shaken 5 times for 5 seconds each using a vortex. Ten-fold dilutions of PBS extracts in peptone water were made ($10^0 \div 10^8$) and inoculations on TSA medium by flooding. The plates were incubated at 37°C for 24 hours. After the incubation, bacterial colonies that grew on Petri plates were counted.

For determination of antimicrobial activity of filaments, cell suspensions containing 1.5×10^7 to 5×10^7 CFU/mL of tested bacterial strain, were placed in separate bottles of 45 mL, followed by addition of 5 g of PCL filament (control sample) or proper CS-CO_2/PVA/PCL filament (tested sample). Then samples were incubated at 37°C for 24 hours in an incubator with constant shaking at 200 rpm (Heidolph Unimax 1010, Merck Sp. z o.o., Warsaw, Poland). After incubation, ten-fold dilutions in peptone water were made ($10^0 \div 10^8$) and inoculations on TSA medium by flooding. The

6

242 plates were incubated at 37°C for 24 hours. After the incubation, bacterial colonies that grew on

243 Petri plates were counted.

244   **The antimicrobial activity of the 3D prints** was evaluatedanalogously to the procedure used

245 for CS-CO$_2$/PVA composites. The test samples were prepared by printing the tiles in a square

246 shape. with a side length of 5 cm and a thickness of 0.5 cm. The negative control was a plaque of

247 the same dimensions printed from PCL.

248   To calculate the number of cells per mL of the initial suspension, the results of the colony counts

249 were used, the number of which, after incubation on the plates, ranged from 30 ÷ 300 units,

250 according to the equation:

251 $$Vc = N \times D,$$

252

253 where Vc is the bacteria concentration, in colony forming units per ml (CFU/mL),N is the average

254 value, in colony forming units (CFU), from Petri dishes, D is the dilution factor from the plates

255 counted. Antimicrobial activity was calculated according to the formula:

256 $$R = \log\frac{B}{C},$$

257 where B is the average of the number of viable cells on the tested sample after 24 h incubation at

258 37°C (CFU/mL), C is the average of the number of viable cells on the control sample after 24 h

259 incubation at 37°C (CFU/mL). A percentage reduction of bacteria/fungi on a logarithmic scale (R)

260 equal to 1, 2, and 3 corresponds to a reduction of 90%, 99%, and 99.9%, respectively.

261 **2.7. Statistical Analysis of the Data**

262 The STATISTICA software (StatSoft, Inc., Tulsa, OK, USA) was used for analyses. The statistical

263 significance was determined at $p < 0.05$. All data reported were based on the means of three

264 replicates ($n = 3$) or five (n=5) replicates in the case of mechanical tests. Experimental results were

265 expressed as mean ± standard deviation (SD). Student's t-test and one-way analysis of variance

266 (ANOVA) were applied. The differences were considered to be statistically significant at $p < 0.05$.

267 **3. Results and discussion**

268 **3.1 Assessment of the effect of temperature treatment on the stability of CS-CO$_2$/PVA**

269 **composites**

270 During visual evaluation of the influence of temperature treatment on the stability of CS-CO$_2$/PVA

271 composites, significant differences in their colour were observed. They resulted from the type of

272 acid used during composites preparation (Fig.1).

7

Acid type	Time [min]			
	0	120	180	240
Acetic				
Hydrochloric				
Carbonic				

273
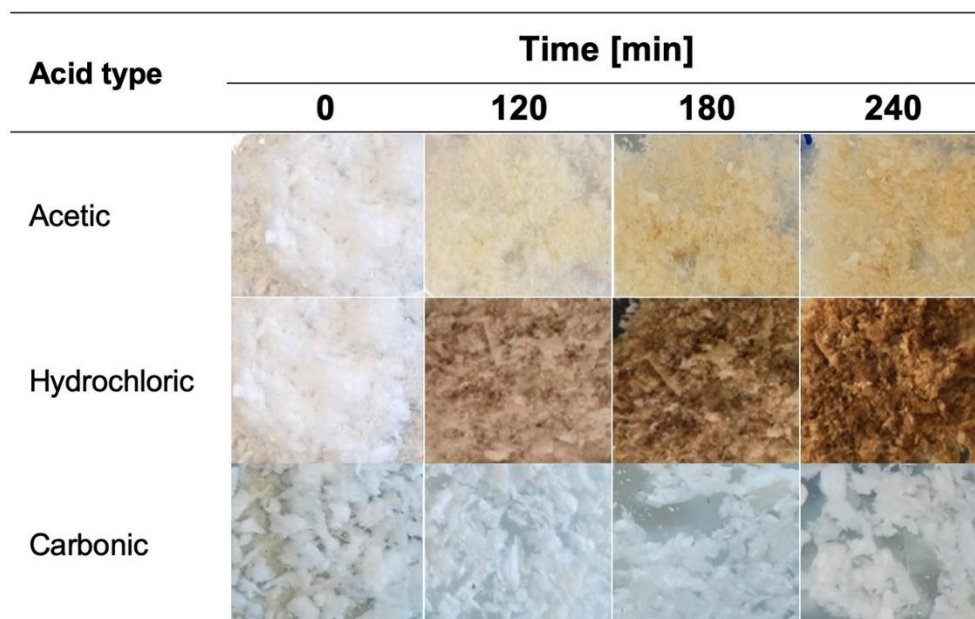
Fig.1. Comparison of color changes of CS-CO$_2$/PVA composites at the ratio of 1:1 m/m heated at 150°C for 4 hours.

The change in the colour of samples indicated the degradation of polymers present in the composite. It is an undesirable phenomenon as it leads to structural changes in polymer chains (e.g. loss of molecular weight) and as a result, changes in the physicochemical and biological properties of the material. In the context of the use of chitosan in various biomaterials, the greatest threats are biodegradation, degradation by ultrasounds, thermal degradation, and photodegradation. The presence of acid in chitosan materials mainly causes the hydrolysis of the polymer to a lower molecular weight without significantly affecting the deacetylation degree and polydispersity (Sikorski, Gzyra-Jagieła, & Draczyński, 2021). The strongest darkening of the composites was observed while using hydrochloric acid. During four hours of heating at 150°C, the colour changed from white to brown. A less intense colour change during heating was shown in the material for which a solution of chitosan in acetic acid was used. After heating this material under the same conditions a change in colour from white to yellow was observed. In the case of composites prepared with chitosan solution in carbonic acid, no effect of temperature on the change of their colour was observed. Grande and co-workers found that the color change of CS/PVA blends is dependent on the drying method, and best results can be obtained by using freeze-drying and spray-drying (an only slightly yellow tone) (Grande et al., 2018). However, subjecting thus dried composites containing at least 25% (m/m) of chitosan to hot-pressing (150°C), still causes their darkening, even if volatile acetic acid was used to dissolve chitosan. Hot-pressed composites did not change their color due to the temperature treatment, when the chitosan content in their composition did not exceed 10% (m/m). The results we presented confirmed that the innovative method of dissolving chitosan with the use of carbon dioxide allowed the creation of thermostable CS-CO$_2$/PVA composites, even if chitosan constitutes as much as 50% of their mass.

3.2. CS-CO$_2$/PVA chemical structure

8

299   The infrared spectroscopy was used to identify individual chemical groups in pure chitosan and

300   PVA as well as to register structural changes in composites of both polymers (Fig. 2). Figure 2.A

301   shows the chitosan spectrum. Intense signals at wavelengths of 1150 cm^{-1}, 1058 cm^{-1}, 1026 cm^{-1}

302   and 893 cm^{-1} indicate the presence of a saccharide structure. Another characteristic band at

303   3349/3301 cm^{-1} is the signal coming from the hydroxyl group of the chitosan molecule. A series of

304   signals at 1652 cm^{-1}, 1557 cm^{-1} and 1315 cm^{-1} correspond to amides I, II and III. The remaining

305   marked signals come from groups $-CH_2-$ (Mania et al., 2019; Staroszczyk, Sztuka, Wolska, Wojtasz-

306   Pająk, & Kołodziejska, 2014).

307   The PVA spectrum is shown in Figure 2.B. Both PVA and chitosan spectra have several analog

308   signals. The signal at about 3342 cm^{-1} corresponds to tensile vibrations of the hydroxyl group, at

309   2917 cm^{-1} and 1426 cm^{-1} to tensile and deformation vibrations of alkyl grups. Other signals

310   characteristic for PVA are in the range 1750-1000 cm^{-1}. For example, the band at 1726 cm^{-1} is a

311   signal of C-O and C=O tensile vibrations of the acetate group. In addition, several signals have

312   been observed which are the result of interactions between PVA mers such as at 1371 cm^{-1} ((OH)-

313   C-OH), 1238 cm-1 (=C-O-C), 1088 cm^{-1} (C-O-C) and 1020 cm^{-1} ((C-O)-C-OH) (Alhosseini et al.,

314   2012; Mansur, Sadahira, Souza & Mansur, 2008).

315   Analyzing the spectrum of PVA/CS composites (Figure 2.C), characteristic peaks were detected

316   as in the spectra of individual components of this composite. Chitosan and PVA do not show strong

317   interactions between each other as evidenced by the lack of new signals and significant shifts of

318   existing peaks. The only shift observed was found in the case of signals corresponding to tensile

319   vibrations of hydroxyl and alkyl groups. Moreover, on the basis of the obtained spectrum it was

320   confirmed that the intensity of its signals increases with the increase of the share in the composition

321   of a given polymer. These results are consistent with the work of Grande and co-workers (Grande
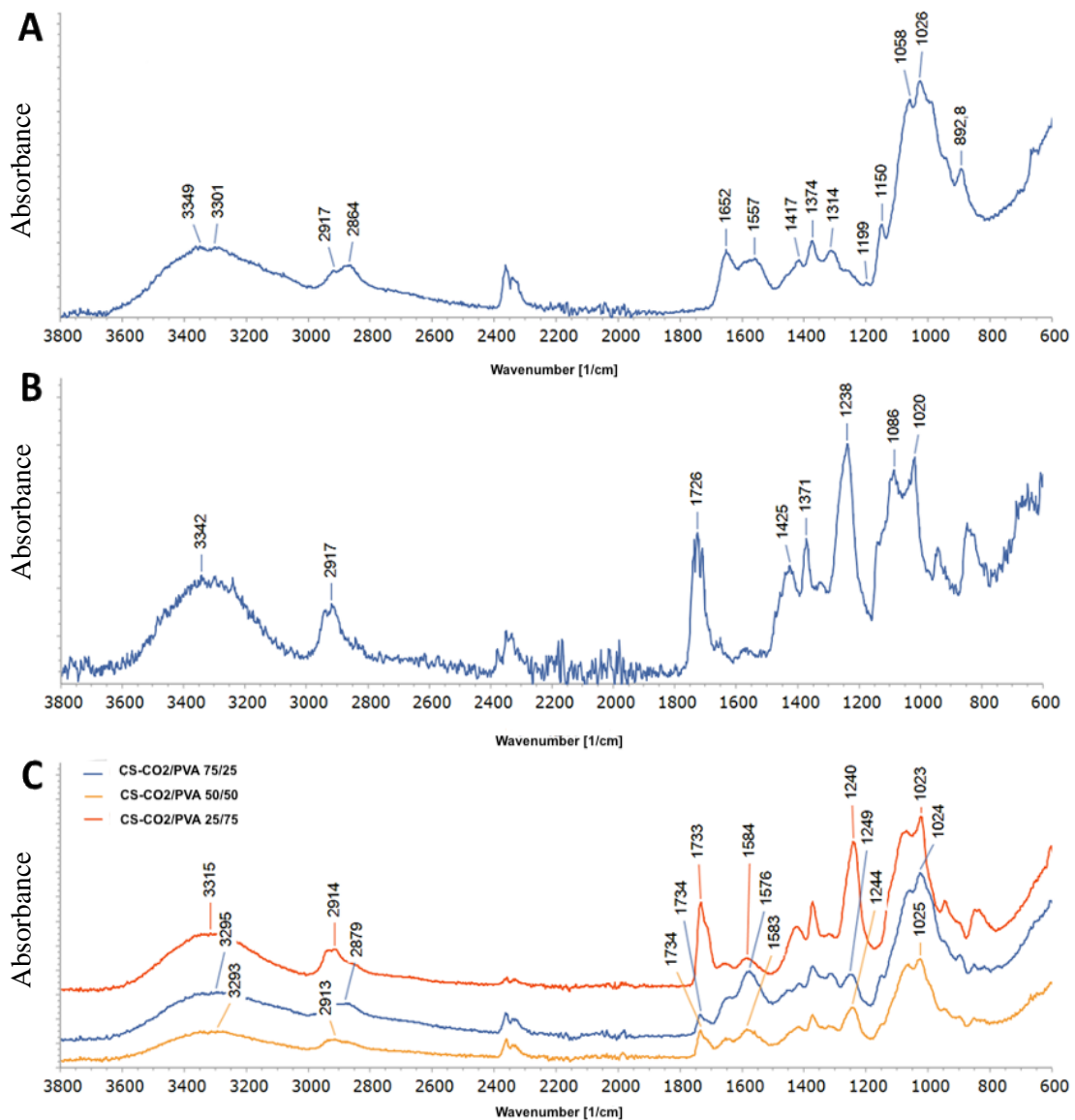
322   et al., 2018).

9

Fig.2. FTIR spectra obtained for CS (A), PVA (B) and PVA/CS (C) composites.

3.3. CS-CO$_2$/PVA/PCL filaments production

PCL was used as the matrix for the production of filaments and doped with one of the three CS-CO$_2$/PVA obtained composite. The 1% solutions of CS-CO$_2$ and PVA were combined to obtain CS-CO$_2$/PVA composites with mass fractions of 75/25, 50/50 and 25/75. The freeze-dried composites subsequently subjected to extrusion are shown in Figure 3.
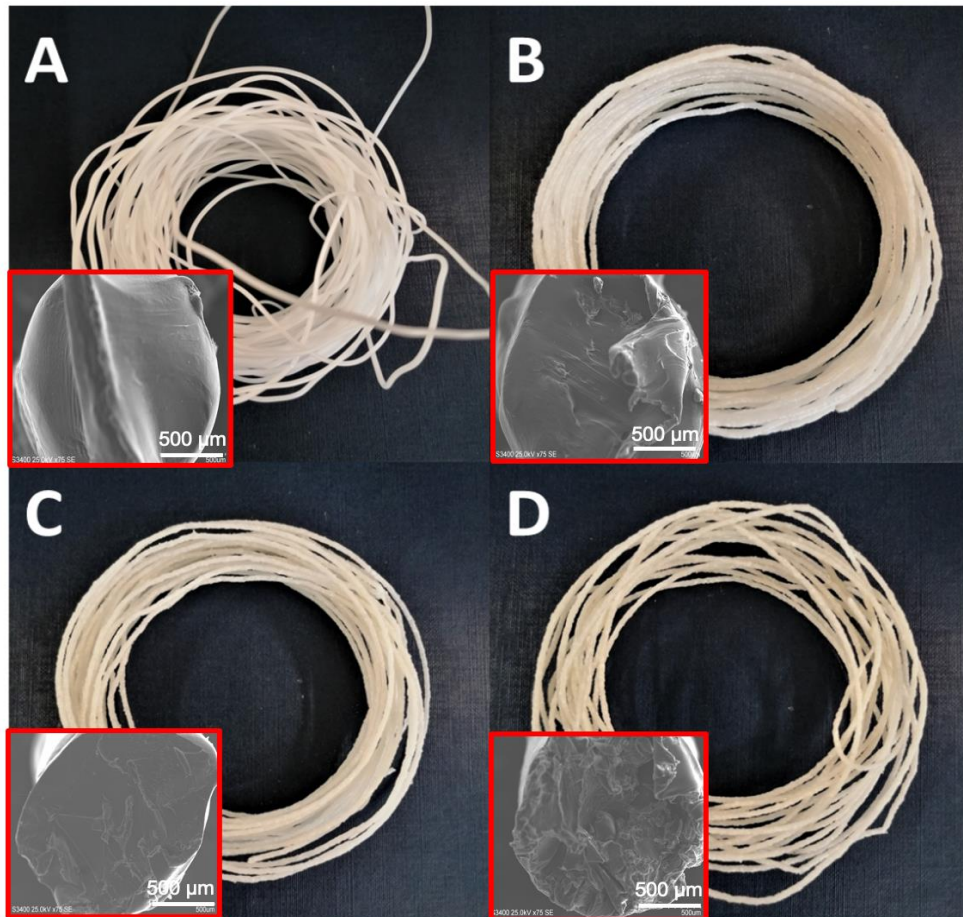
Fig. 3. Granules obtained by combining CS-CO$_2$ and PVA solutions, freeze drying and extrusion (150°C) at mass ratios 25/75 (A), 50/50 (B) and 75/25 (C).

Filaments obtained by extrusion PCL with 20% addition of CS-CO$_2$ composite are shown in Figure 4.

Fig. 4. Photographs and SEM micrographs of CS-CO$_2$/PVA/PCL filaments at mass ratios: 0/0/100 (A), 5/15/80 (B), 10/10/80 (C), 15/5/80 (D).

Based on SEM micrographs, it was observed that the filaments became less homogeneous with increasing chitosan concentration. They have a more coarser structure compared to the filament obtained exclusively from PCL granules. The increase in filament heterogeneity with the increase in chitosan concentration was also observed in our previous work, where PLA was used as the base

11

342 thermoplastic material. Due to the lack of the compatibilizer in the form of PVA, the deposition of

343 chitosan in the PLA matrix resulted in the formation of large pores in the filament and air pockets,

344 when the chitosan concentration was 10% (Mania et al., 2019). The use of PVA prevents such

345 problems, even when chitosan constitutes 15% of the filament's weight. Grande et al (2015)

346 demonstrated that the use of freeze-drying in the formation of PVA/chitosan composites significantly

347 improves the dispersion of these composites in PLA. The evidence is the observed particle size

348 distribution and a reduction in the dispersed particle reaching 0.5–5 µm during the

349 thermomechanical mixing process, as demonstrated by the SEM analysis (Grande et al., 2015). In

350 our investigation we observed that increase of the chitosan content in CS-CO$_2$/PVA composite

351 caused the worst distribution and the worst homogenity of the material. For CS-CO$_2$/ PVA

352 composite containing 25%, 50%, and 75% of chitosan (m/m), the particle distribution was in the

353 range 5 -10 µm, 25 - 40 µm, and 50 - 60 µm, respectively (*Supplementary materials*). Chen and

354 colleagues suggested that particle distribution is associated with hydrogen bonds between the

355 hydroxyl groups of PVA and the amino groups of chitosan. Increasing the chitosan content in the

356 material increases the the level of ionic cross-linking tended to form the bigger CS/PVA particle

357 agglomerates (Chen et al., 2017). This understanding matches the results obtained for filaments

358 using the SEM technique (Fig. 4).

359 3.4. Thermal stability

360 The thermograms, derivative weight plots of CS-CO$_2$/PVA/PCL and their components are

361 presented in figure 5. The TGA curve of chitosan exhibited an endothermic effect attributable to water

362 release at the range 25-145°C (Fig. 5A) with 13.1% weight loss. The second decomposition stage is

363 attributed to a complex process including dehydratation of saccharide rings, depolymerization and

364 decomposition of the acethylated units of the polymer (42.0% weght loss) (Lewandowska, 2009;

365 Moussout, Ahlafi, Aazza & Bourakhouadar, 2016). According to Eulalio and others, the third

366 decomposition stage (measured for chitosan powder) is a thermo-oxidative process that starts at

367 approx. 500°C, with maximum velocity at approx. 600°C and a weight loss of 40-45%, leaving no

368 residue behind (Eulalio, Rodrigues, Santos, Peniche, & LiaFook, 2019) . In our tests, there was also

369 a loss in weight that occurred above 400°C continuously with a small offset at 740°C (Fig.5A). The

370 PVA curve consisted of three stages (Fig. 5B). The first weight loss at 20-120°C is related to moisture

371 vaporization (4% weight loss). The second occurs at 305°C with 75% weight loss due to dehydration

372 of the chain with the release of volatile compounds. The last stage of weight loss above 400°C is

373 caused by degradation of polyene residues with formation of carbon and hydrocarbon (Lewandowska,

374 2009; Raju, Rao, Reddy, & Veera Brahmam, 2007). The TGA curve of PCL shows only one stage of

375 mass loss due to the lack of water absorption capacity of this polymer. In the temperature range from

376 350°C to 420°C almost complete weight loss due to depolymerization with the formation of ε-

377 caprolactone, which is subject to further decomposition is observed (Aoyagi, Yamashita, & Doi, 2002).

378 In turn, the TGA curves of CS-CO$_2$/PVA/PCL filaments were characterized by only one stage of

379 decomposition, during which almost complete loss of mass occurred (Fig. 5.D-F). Both the curve

380 course and the temperature value range for the stage of greatest mass loss coincide with the TGA

381 PCL curve. The results of the thermal analysis confirm the results of the visual assessment of the CS-

382 CO$_2$/PVA composites (Fig. 1). The PCL degradation starts above 350°C, so any loss of filament

12

weight until the printing temperature is reached may result from changes in chitosan and PVA. However, the weight loss of all produced filaments up to 150°C did not exceed 2% which suggests that the composites do not absorb nearly as much water as the CS and PVA materials. (Fig. 5 D-F). The weight loss measured up to 150°C for chitosan, PVA and CS-CO_2/PVA composites containing 25%, 50% and 75% chitosan, was 18%, 5%, 5%, 7%, 10%, respectively. Thermograms for CS-CO_2/PVA composites are found in the *Supplementary materials* file. The decomposition temperature of them appears to shift from 275°C towards 225°C with increasing CS content. This is above the extrusion and printing temperature of 150°C, but is consistent with decomposition temperatures of 275°C for PVA and 225°C for CS.
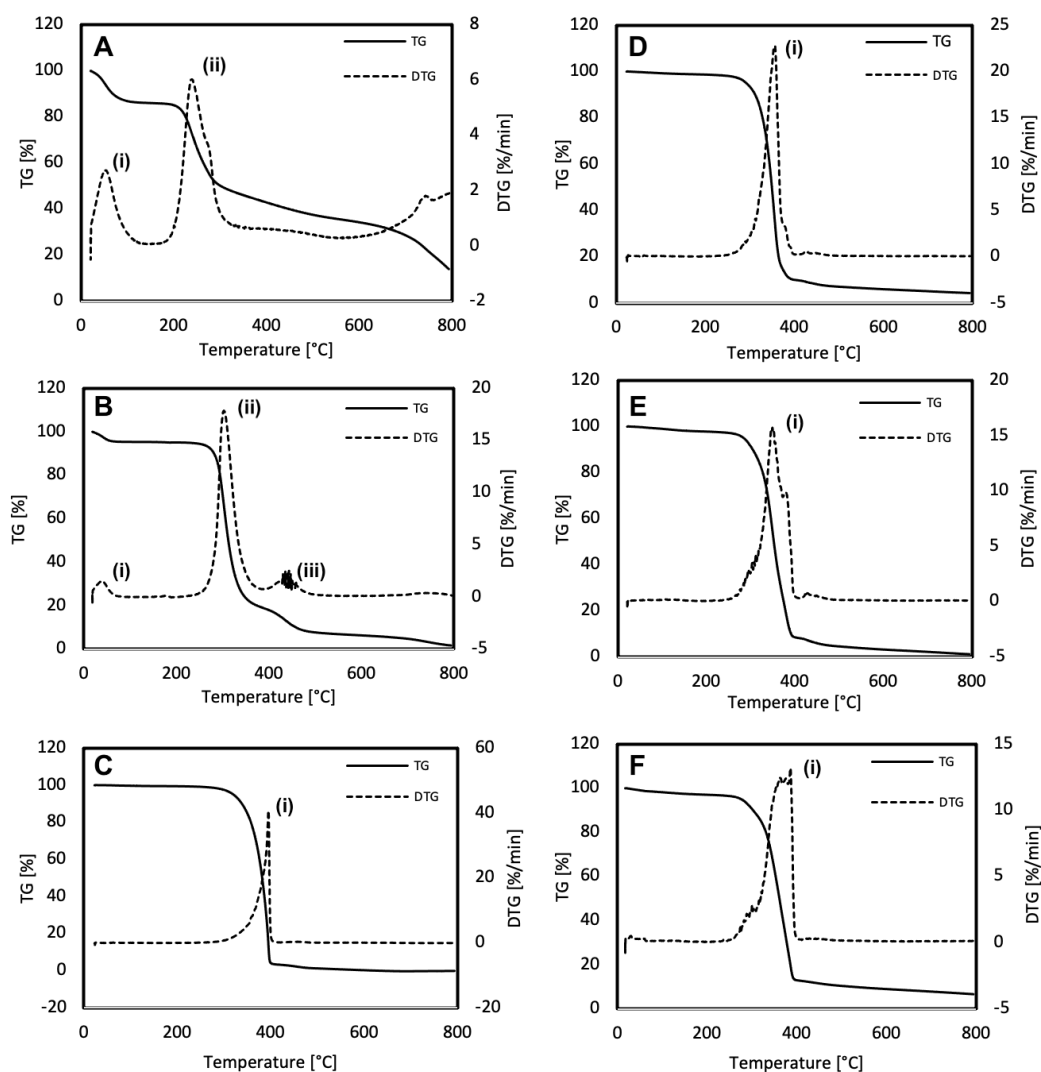
Fig. 5. TGA and TGA derivative curves of chitosan (A) CS, (B) PVA, (C) PCL, (D) CS-CO_2/PVA/PCL filament with 5/15/80 components ratio, (E) CS-CO_2/PVA/PCL filament with 10/10/80 components ratio, (F), CS-CO_2/PVA/PCL filament with 15/5/80 components ratio.

3.5. Mechanical properties and printability

The comparison of the filaments printability, mechanical properties of filaments and 3D prints obtained from them are presented in Table 1. The obtained CS-CO_2/PVA/PCL filaments were subjected to

13

mechanical tensile tests to determine the following parameters: tensile strength, elongation at break and Young's modulus. Based on the obtained results, significant differences between pure PCL and subsequent CS-CO$_2$/PVA/PCL samples with different chitosan content were found. The addition of the filler in the form of the CS-CO$_2$/PVA composite decreased the tensile strength by 73.6%, 67.8% and 56.6%, in relation to the PCL value, when the chitosan content in the filament was 5%, 10% and 15%, respectively. Filaments containing chitosan had 50-64% lower extension at break value and 50-75% lower Young modulus than the PCL filament. Deterioration of the mechanical properties of filaments with an increase in chitosan concentration was also observed in our previous work (Mania et al., 2019). Reduction in tensile strength by about 60% in PLA filaments with addition of 10% chitosan corresponded to the same reduction in tensile strength of CS-CO$_2$/PVA/PCL filaments with a 15/5/80 ratio. The equal reduction in tensile strength even at 5% higher concentration of chitosan in thermoplastic filaments may be due to the use of PVA as a compatibilizer in the physical mixture of raw materials. Filaments containing a filler in the form of a composite of chitosan with PVA, in relation to filaments only with the addition of chitosan, but at a similar concentration of this polymer, are characterized by lower elongation ability (Mania et al., 2019). Based on Young modulus-tensile strength chart, all obtained CS-CO$_2$/PVA/PCL filaments are classified as natural materials (Shah, 2014). Properties closest to thermoplastic materials were demonstrated by a filament with addition of 15% chitosan. To be included in this group, the same filament should have approx. 2.7 times greater tensile strength with recent Young modulus.

Despite the significant deterioration of the mechanical parameters of the filaments resulting from the use of the CS-CO$_2$/PVA composite filler in the PCL matrix, all filaments obtained can be described as printable. They fall within the printability window described in the experiment of Xu and colleagues: > 80 kg/mm^2*% (Xu et al., 2020). The printability of the filaments demonstrated in the instrumental test was confirmed in a printout using a 3D FDM printer (Fig.6).

Table 1. Comparison of the filaments' printability, their mechanical properties and 3D prints obtained from them (n=10, p<0.05).

Material type	PCL	CS-CO$_2$/PVA/PCL 5/15/80	CS-CO$_2$/PVA/PCL 10/10/80	CS-CO$_2$/PVA/PCL 15/5/80
Filament				
Tensile strength [MPa]	21.49 ± 1.02[a]	5.68 ± 0.15[b]	6.91 ± 0.21[c]	9.32 ± 0.43[d]
Extension at break [%]	21.96 ± 0.79[a]	10.89 ± 0.30[b]	10.34 ± 0.44[b]	7.83 ± 0.19[c]
Young modulus [MPa]	15.50 ± 0.48[a]	8.03 ± 0.50[b]	6.22 ± 0.18[c]	3.98 ± 0.09[d]
Printability [kg/mm^2*%]	187.9 ± 3.2[a]	131 ± 2.0[b]	103.1 ± 1.4[c]	95.3 ± 1.1[d]
3D print				
Hardness [kPa]	3.42 ± 0.08[a]	3.95 ± 0.06[b]	4.35 ± 0.09[c]	4.67 ± 0.04[d]
Flexibility [-]	0.88 ± 0.03[a]	0.72 ± 0.05[b]	0.69 ± 0.03[b]	0.57 ± 0.02[c]
Cohesiveness [-]	0.73 ± 0.05[a]	0.70 ± 0.04[a]	0.62 ± 0.06[a]	0.65 ± 0.02[a]

Values with different letters marked from a to d differ significantly from the control sample in each row.

Compression tests have shown that increasing the chitosan concentration in the printout increases its hardness and decreases and its flexibility. The samples with addition of 5%, 10% and 15% chitosan were 15.5%, 27.2% and 36.5% harder and 18.2%, 21.6% and 35.2% less flexible compared to PCL,respectively. The addition of chitosan did not significantly affect the cohesiveness of the 3D prints, which was comparable to that of the prints made of polycaprolactone (Table 1). Visually, there was no difference between the samples.

14

433 Fig.6. The photography of 3D objects in the form of cylinders printed with the FDM method from the obtained

435 composite filaments (from the left 3D prints containinng 5%, 10% and 15% of chitosan).

436 **3.6. Antimicrobial properties**

437 To evaluate the antimicrobial properties of the filaments the ASTM: E2149 method with slight

438 modifications was used, which is designed to measure the antimicrobial activity of non-leaching

439 (non-water soluble) antimicrobials surfaces made of plastic, rubber, silicone, and treated fabric

440 material and is one method to test an irregularly shaped antimicrobial object, such as a thread,

441 powder or 3D molded plastic. The results of the antimicrobial activity tests are presented in the form

442 of the degree of reduction obtained after 24-hour contact of *S. aureus* and *E.coli* inoculum with the

443 tested materials. PCL and PVA have no antimicrobial properties (Aslam, Kalyar, & Raza, 2018;

444 Balcucho, Narváez, & Castro-Mayorga, 2020). It was found that all CS-CO$_2$/PVA composites had

445 the strongest antimicrobial effect against *S. aureus* and *E. coli (*at least 2 log orders which

446 corresponds to 99% reduction*),* compared to PCL filaments and prints. This activity also increased

447 for both bacterial strains along with an increase in chitosan concentration in the material (Fig.7.)

448 The highest value was recorded for CS-CO$_2$/PVA composites containing 75% of chitosan against a

449 *S. aureus* strain. The same composite also caused the strongest antimicrobial effect after being

450 used to produce filaments and for 3D printing. The greater antimicrobial effect of the CS-CO$_2$/PVA

451 composite, CS-CO$_2$/PVA/PCL filaments and 3D prints was obtained with respect to the Gram-

452 positive strain. The 3D prints showed virtually the same antimicrobial properties as the filaments

453 from which they were printed. It means that re-melting the CS-CO$_2$/PVA/PCL material has no

454 significant effect on the inhibition of the material's antimicrobial activity. The antimicrobial activity

455 was due to the presence of chitosan and depends on the degree of its deacetylation, molecular

456 weight, concentration in solution, pH, and ionic strength of the solution (Rinaudo, 2006). According

457 to Goy and colleagues, there is a lack of conclusive data on whether chitosan has higher activity on

458 Gram-positive or on Gram-negative bacteria (Goy, de Britto, & Assis, 2009). On both strains,

459 chitosan seems to act differently, though in both cases satisfactorily. The main reason for the

460 antimicrobial activity of chitosan is the interaction of its positively charged chains with anionic

461 components of microorganisms—lipopolysaccharides (Gram-negative bacteria) and teichoic acids

15

462 (Gram-positive bacteria) that cause bacterial cell lysis. However, this mechanism takes place when
463 the amino groups of the polymer are protonated: pH < 6 (Kong, Chen, Xing, & Park, 2010).

A
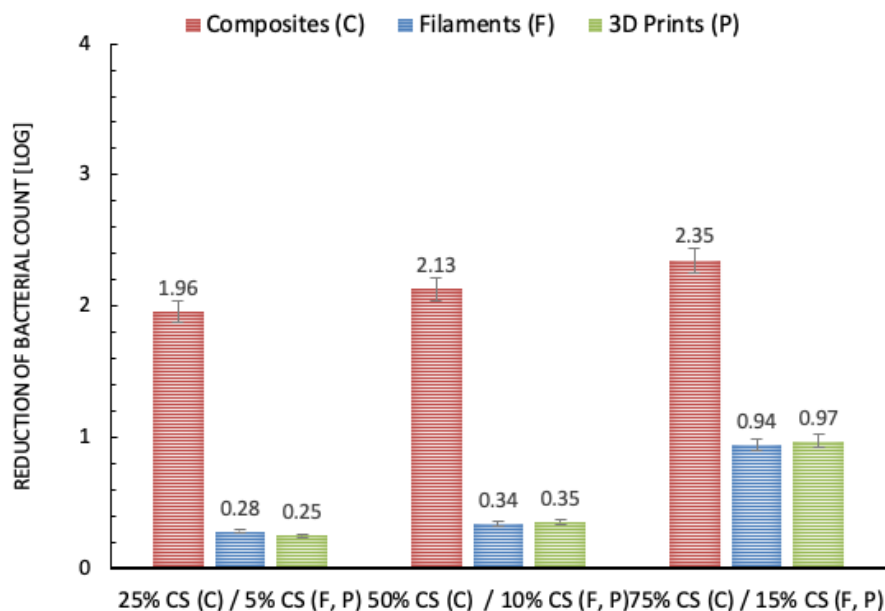
B
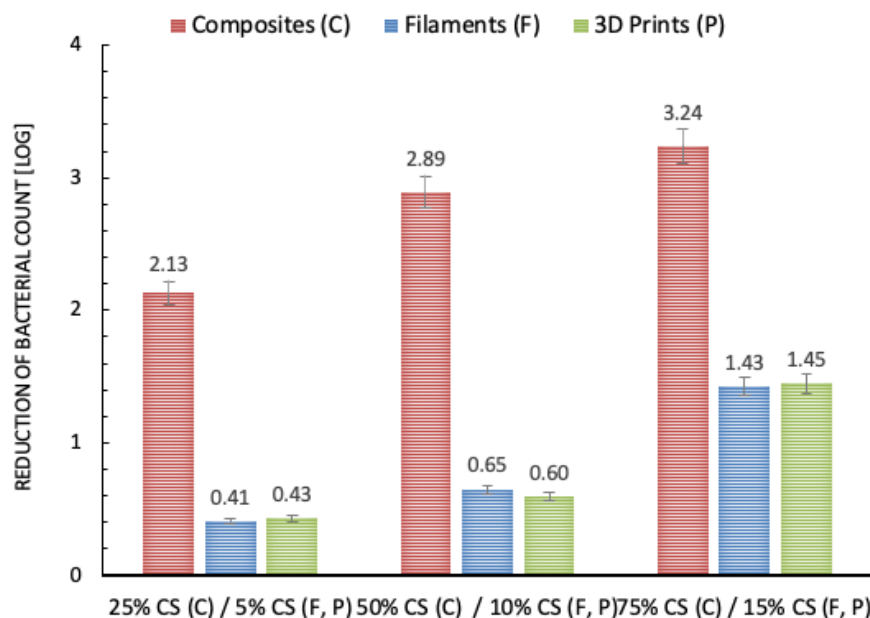
464

465 Fig. 7. The antimicrobial activity against (A) *E. coli* and (B) *S.aureus* of CS-CO$_2$/PVA composites, and CS-
466 CO$_2$/PVA/PCL filaments and prints estimated according to Standard ASTM: E2149.

467 It has been concluded that for neutral or alkaline media, the cationic nature of chitosan can no
468 longer explain its antibacterial activity. In this case, the strong coordination capability of –NH$_2$

16

469 groups in the chitosan chain might be one possible mechanism (Mania et al., 2018; Xie, Wang, &

470 Liu, 2002).

471 In the scientific literature, it has been confirmed that the antimicrobial activity of chitosan does not

472 imply a cytotoxic effect. Da Silva and co-workers used chitosan from the same producer and with

473 the same parameters to obtain scaffolds for cartilage tissue engineering. They confirmed that the

474 viability of the chondrocytes from pig stifles estimated by the live / dead assay did not differ between

475 the four groups of chitosan scaffolds and was above 80% (Da Silva et al., 2016). Moreover, in the

476 earlier work of our team it was shown that chitosan hydrogels obtained by the CO_2 saturation

477 method are characterized by higher biocompatibility towards mouse NIH 3T3 fibroblasts,

478 than their counterparts in solutions of organic or mineral acids (Gorczyca et al., 2014). Also no

479 cytotoxic effect was noted for polycaprolactone and polyvinyl alcohol (Ragetly et al., 2010; Zhang et

480 al., 2019)

481 **4. Conclusion**

482 In our work we present an innovative method for processing chitosan in a thermoplastic matrix.The

483 use of the CO_2 saturation technique in the preparation of CS-CO_2/PVA composites allows

484 generation of a polar filler for thermoplastics containing up to 75% chitosan. So far, such a solution

485 has not been presented by any research team and it overcame the limitation previously described in

486 the literature regarding the presence of residual solvents. The use of a 20% filler addition in a

487 thermoplastic material allows it to achieve a chitosan concentration in the range of 5-15% m / m,

488 and to produce a filament suitable for use in 3D printing with the FDM technology. Both, CS-

489 CO_2/PVA/PCL filaments and prints are characterized by antimicrobial activity against gram negative

490 and gram positive indicator bacteria. This activity depends on the concentration of chitosan and

491 ensure reduction of bacterial growth even above 0.94 in logarithmic scale (89%) in the case of

492 materials containing 15% of chitosan. The filler decreases the mechanical properties of the

493 filaments, but it does not significantly affect their printability. On the other hand, 3D prints become

494 harder, less flexible and consistent with increasing chitosan concentration. The absence of acid in

495 the materials allows the thermal stability of the filaments to be ensured, which is extremely

496 important in its further processing, including in 3D printing conditions.The presented results may

497 have great potential in biological applications as cell growth scaffolds, including in regenerative

498 medicine.

512 **References**

513 Alhosseini, S. N., Moztarzadeh, F., Mozafari, M., Asgari, S., Dodel, M., Samadikuchaksaraei, A.,
514   Kargozar, S., & Jalali, N. (2012). Synthesis and characterization of electrospun polyvinyl
515   alcohol nanofibrous scaffolds modified by blending with chitosan for neural tissue engineering.
516   *International Journal of Nanomedicine*, *7*, 25–34.

517 Aoyagi, Y., Yamashita, K., & Doi, Y. (2002). *Thermal degradation of poly [(R) -3-hydroxybutyrate],*
518   *poly [e -caprolactone], and poly [(S) -lactide]. 76*, 53–59.

519 Aslam, M., Kalyar, M. A., & Raza, Z. A. (2018). Polyvinyl alcohol: A review of research status and
520   use of polyvinyl alcohol-based nanocomposites. *Polymer Engineering & Science*, *58*, 2119–
521   2132.

522 Balcucho, J., Narváez, D. M., & Castro-Mayorga, J. L. (2020). Antimicrobial and biocompatible
523   polycaprolactone and copper oxide nanoparticle wound dressings against methicillin-resistant
524   staphylococcus aureus. *Nanomaterials*, *10*(9), 1–21. https://doi.org/10.3390/nano10091692

525 Bi, L., Cao, Z., Hu, Y., Song, Y., Yu, L., Yang, B., Mu, J., Huang, Z., & Han, Y. (2011). Effects of
526   different cross-linking conditions on the properties of genipin-cross-linked chitosan/collagen
527   scaffolds for cartilage tissue engineering. *Journal of Materials Science: Materials in Medicine*,
528   *22*(1), 51–62. https://doi.org/10.1007/s10856-010-4177-3

529 Bonilla, J., Fortunati, E., Vargas, M., Chiralt, A., & Kenny, J. M. (2013). *Accepted Manuscript.*

530 Chen, Q., Liu, Y., Wang, T., Wu, J., Zhai, X., Li, Y., Lu, W. W., Pan, H., & Zhao, X. (2017).
531   Chitosan-PVA monodisperse millimeter-sized spheres prepared by electrospraying reduce the
532   thromboembolic risk in hemorrhage control. *Journal of Materials Chemistry B*, *5*(20), 3686–
533   3696. https://doi.org/10.1039/c7tb00032d

534 Correlo, V. M., Boesel, L. F., Pinho, E., Costa-Pinto, A. R., Alves Da Silva, M. L., Bhattacharya, M.,
535   Mano, J. F., Neves, N. M., & Reis, R. L. (2009). Melt-based compression-molded scaffolds
536   from chitosan-polyester blends and composites: Morphology and mechanical properties.
537   *Journal of Biomedical Materials Research - Part A*, *91*(2), 489–504.
538   https://doi.org/10.1002/jbm.a.32221

539 Da Silva, A. R. P., Macedo, T. L., Coletta, D. J., Feldman, S., & Pereira, M. de M. (2016). Synthesis,
540   characterization and cytotoxicity of Chitosan/Polyvinyl alcohol/bioactive glass hybrid scaffolds
541   obtained by Lyophilization. *Revista Materia*, *21*(4), 964–973. https://doi.org/10.1590/S1517-
542   707620160004.0089

543 Dang, K. M., & Yoksan, R. (2015). Development of thermoplastic starch blown film by incorporating
544   plasticized chitosan. *Carbohydrate Polymers*, *115*, 575–581.
545   https://doi.org/10.1016/j.carbpol.2014.09.005

546 Epure, V., Griffon, M., Pollet, E., & Avérous, L. (2011). Structure and properties of glycerol-
547   plasticized chitosan obtained by mechanical kneading. *Carbohydrate Polymers*, *83*(2), 947–
548   952. https://doi.org/10.1016/j.carbpol.2010.09.003

549 Eulalio, H. Y. C., Rodrigues, J. F. B., Santos, K. O., Peniche, C., & LiaFook, M. V. (2019).
550   Characterization and. thermal properties of chitosan films prepared with different acid
551   solvents. *Revista Cubana de Química*, *31*, 309–323.

552 Gorczyca, G., Tylingo, R., Szweda, P., Augustin, E., Sadowska, M., & Milewski, S. (2014).
553   Preparation and characterization of genipin cross-linked porous chitosan-collagen-gelatin
554   scaffolds using chitosan-CO_2 solution. *Carbohydrate Polymers*, *102*(1), 901–911.
555   https://doi.org/10.1016/j.carbpol.2013.10.060

556 Goy, R. C., De Britto, D., & Assis, O. B. G. (2009). A review of the antimicrobial activity of chitosan.
557   *Polimeros*, *19*(3), 241–247. https://doi.org/10.1590/S0104-14282009000300013

558 Grande, R., Pessan, L. A., & Carvalho, A. J. F. (2015). Ternary melt blends of poly(lactic
559   acid)/poly(vinyl alcohol)-chitosan. *Industrial Crops and Products*, *72*, 159–165.

560 Grande, R., Pessan, L. A., & Carvalho, A. J. F. (2018). Thermoplastic blends of chitosan: A method
561   for the preparation of high thermally stable blends with polyesters. *Carbohydrate Polymers*,
562   *191*(December 2017), 44–52. https://doi.org/10.1016/j.carbpol.2018.02.087

563 Hoyer, B., Bernhardt, A., Heinemann, S., Stachel, I., Meyer, M., & Gelinsky, M. (2012).
564   Biomimetically mineralized salmon collagen scaffolds for application in bone tissue
565   engineering. *Biomacromolecules*, *13*(4), 1059–1066. https://doi.org/10.1021/bm201776r

566 Kong, M., Chen, X. G., Xing, K., & Park, H. J. (2010). Antimicrobial properties of chitosan and mode
567   of action: A state of the art review. *International Journal of Food Microbiology*, *144*(1), 51–63.
568   https://doi.org/10.1016/j.ijfoodmicro.2010.09.012

569 Lewandowska, K. (2009). Miscibility and thermal stability of poly(vinyl alcohol)/chitosan mixtures.
570   *Thermochimica Acta*, *493*(1–2), 42–48. https://doi.org/10.1016/j.tca.2009.04.003

571 Mania, S., Ryl, J., Jinn, J.-R., Wang, Y.-J., Michałowska, A., & Tylingo, R. (2019). The production
572   possibility of the antimicrobial filaments by co-extrusion of the pla pellet with chitosan powder
573   for FDM 3D printing technology. *Polymers*, *11*(11). https://doi.org/10.3390/polym11111893

574 Mania, S., Tylingo, R., Augustin, E., Gucwa, K., Szwacki, J., & Staroszczyk, H. (2018). Investigation
575   of an elutable N-propylphosphonic acid chitosan derivative composition with a chitosan matrix
576   prepared from carbonic acid solution. *Carbohydrate Polymers*, *179*.
577   https://doi.org/10.1016/j.carbpol.2017.09.082

578 Mania, Szymon, Banach, A., & Tylingo, R. (2020). Review of current research on chitosan as a raw
579   material in three-dimensional printing technology in biomedical applications. *Progress on
580   Chemistry and Application of Chitin and Its Derivatives*, *25*, 37–50.
581   https://doi.org/10.15259/PCACD.25.003

582 Mansur, H. S., Sadahira, C. M., Souza, A. N., & Mansur, A. A. P. (2008). FTIR spectroscopy
583   characterization of poly (vinyl alcohol) hydrogel with different hydrolysis degree and chemically
584   crosslinked with glutaraldehyde. *Materials Science and Engineering C*, *28*(4), 539–548.
585   https://doi.org/10.1016/j.msec.2007.10.088

586 Matet, M., Heuzey, M. C., Pollet, E., Ajji, A., & Avérous, L. (2013). Innovative thermoplastic chitosan
587   obtained by thermo-mechanical mixing with polyol plasticizers. *Carbohydrate Polymers*, *95*(1),
588   241–251. https://doi.org/10.1016/j.carbpol.2013.02.052

589 Mendes, J. F., Paschoalin, R. T., Carmona, V. B., Sena Neto, A. R., Marques, A. C. P., Marconcini,
590   J. M., Mattoso, L. H. C., Medeiros, E. S., & Oliveira, J. E. (2016). Biodegradable polymer

19

591   blends based on corn starch and thermoplastic chitosan processed by extrusion.

592   *Carbohydrate Polymers*, *137*, 452–458. https://doi.org/10.1016/j.carbpol.2015.10.093

593   Moussout, H., Ahlafi, H., Aazza, M., & Bourakhouadar, M. (2016). Kinetics and mechanism of the

594   thermal degradation of biopolymers chitin and chitosan using thermogravimetric analysis.

595   *Polymer Degradation and Stability*, *130*, 1–9.

596   https://doi.org/10.1016/j.polymdegradstab.2016.05.016

597   Muzzarelli, R. A. A. (2009). Chitins and chitosans for the repair of wounded skin, nerve, cartilage

598   and bone. *Carbohydrate Polymers*, *76*(2), 167–182.

599   https://doi.org/10.1016/j.carbpol.2008.11.002

600   Ngo, T. D., Kashani, A., Imbalzano, G., Nguyen, K. T. Q., & Hui, D. (2018). Additive manufacturing

601   (3D printing): A review of materials, methods, applications and challenges. *Composites Part B:*

602   *Engineering*, *143*(December 2017), 172–196.

603   https://doi.org/10.1016/j.compositesb.2018.02.012

604   Ragetly, G. R., Slavik, G. J., Cunningham, B. T., Schaeffer, D. J., & Griffon, D. J. (2010). Cartilage

605   tissue engineering on fibrous chitosan scaffolds produced by a replica molding technique.

606   *Journal of Biomedical Materials Research - Part A*, *93*(1), 46–55.

607   https://doi.org/10.1002/jbm.a.32514

608   Rajeswari, A., Sreerag Gopi, E., Christy, J. S., Jayaraj, K., & Pius, A. (2020). Current research on

609   the blends of chitosan as new biomaterials. In T. Sabu, A. Pius, & S. Gopi (Eds.), *Handbook of*

610   *Chitin and Chitosan* (1st ed., pp. 248–275). Elsevier Inc. https://doi.org/10.1016/B978-0-12-

611   817970-3.00009-2

612   Raju, C. H. L., Rao, J. L., Reddy, B. C. V., & Brahmam, K. V. (2007). Thermal and IR studies on

613   copper doped polyvinyl alcohol. *Bulletin of Materials Science*, *30*(3), 215–218.

614   https://doi.org/10.1007/s12034-007-0038-1

615   Rinaudo, M. (2006). Chitin and chitosan: Properties and applications. *Progress in Polymer Science*

616   *(Oxford)*, *31*(7), 603–632. https://doi.org/10.1016/j.progpolymsci.2006.06.001

617   Rojas-Martínez, L. E., Flores-Hernandez, C. G., López-Marín, L. M., Martinez-Hernandez, A. L.,

618   Thorat, S. B., Reyes Vasquez, C. D., Del Rio-Castillo, A. E., & Velasco-Santos, C. (2020). 3D

619   printing of PLA composites scaffolds reinforced with keratin and chitosan: Effect of geometry

620   and structure. *European Polymer Journal*, *141*(August), 1–10.

621   https://doi.org/10.1016/j.eurpolymj.2020.110088

622   Shah, D. U. (2014). Natural fibre composites : Comprehensive Ashby-type materials. *Materials &*

623   *Design*, *62*(May), 21–31.

624   Sikorski, D., Gzyra-Jagieła, K., & Draczyński, Z. (2021). The kinetics of chitosan degradation in

625   organic acid solutions. *Marine Drugs*, *19*(5), 1–16. https://doi.org/10.3390/md19050236

626   Staroszczyk, H., Sztuka, K., Wolska, J., Wojtasz-Pająk, A., & Kołodziejska, I. (2014). Interactions of

627   fish gelatin and chitosan in uncrosslinked and crosslinked with EDC films: FT-IR study.

628   *Spectrochimica Acta - Part A: Molecular and Biomolecular Spectroscopy*, *117*, 707–712.

629   https://doi.org/10.1016/j.saa.2013.09.044

630 Xie, W., Xu, P., Wang, W., & Liu, Q. (2002). Preparation of water-soluble chitosan derivatives and
631 their antibacterial activity. *Journal of Applied Polymer Science*, *85*(7), 1357–1361.
632 https://doi.org/10.1002/app.10424

633 Xu, P., Li, J., Meda, A., Osei-Yeboah, F., Peterson, M. L., Repka, M., & Zhan, X. (2020).
634 Development of a quantitative method to evaluate the printability of filaments for fused
635 deposition modeling 3D printing. *International Journal of Pharmaceutics*, *588*(May), 119760.
636 https://doi.org/10.1016/j.ijpharm.2020.119760

637 Zhang, Z. Z., Zhang, H. Z., & Zhang, Z. Y. (2019). 3D printed poly(ε-caprolactone) scaffolds function
638 with simvastatin-loaded poly(lactic-co-glycolic acid) microspheres to repair load-bearing
639 segmental bone defects. *Experimental and Therapeutic Medicine*, *17*(1), 79–90.
640 https://doi.org/10.3892/etm.2018.6947

641